Compressibility Divergence and the Finite Temperature Mott Transition

G. Kotliar,[1] Sahana Murthy,[1] and M. J. Rozenberg[2]

[1]*Serin Physics Laboratory, Rutgers University, 136 Frelinghuysen Road, Piscataway, New Jersey 08854*

[2]*Departamento de Física, FCEN, Universidad de Buenos Aires, Ciudad Universitaria Pab. I, 1428 Buenos Aires, Argentina*

(Received 31 October 2001; published 3 July 2002)

In the context of the dynamical mean-field theory (DMFT) of the Hubbard model, we study the behavior of the compressibility near the density driven Mott transition at finite temperatures. We demonstrate this divergence using DMFT and quantum Monte Carlo simulations in the one-band and the two-band Hubbard model. We supplement this result with considerations based on the Landau theory framework, and discuss the relevance of our results to the α-γ end point in cerium.

DOI: 10.1103/PhysRevLett.89.046401 PACS numbers: 71.10.Fd, 71.27.+a, 71.30.+h

The Mott transition, namely, the metal-insulator transition (MIT) driven by electron-electron interactions [1], is a fascinating phenomenon realized experimentally in many compounds such as V_2O_3 and $Ni(Se, S)_2$ [2]. The Mott transition concept is also relevant to elements in the lanthanide and actinide series [3]. Viewed from a broader perspective, the Mott transition problem forces us to develop tools to describe materials where the electron is not fully described by either a real space picture or a momentum space picture, and continues to spur advances in many body and electronic structure methods.

On the theory side, the Hubbard model is the simplest Hamiltonian that captures some of the essential physics of the transition. It has been intensively studied in one dimension, but in this limit no finite temperature phase transition can take place. In recent years, theoretical progress has been made in the understanding of the Mott-Hubbard transition using the DMFT [4]. In this framework, the transition can be viewed as bifurcation points of a functional [5,6] of the local Green's function, or of its conjugate variable, the Weiss field which describes the local environment of a correlated site.

The case of the correlation strength (U) driven MIT at half filling (particle-hole symmetric case) is now well understood. At temperature $T = 0$, there are two bifurcation points, one denoted by $U_{c1}(T = 0)$, where the insulating solution disappears, and the other denoted by $U_{c2}(T = 0)$, where the metallic state disappears in a fashion reminiscent of the Brinkman-Rice scenario [7]. As shown in the inset of Fig. 1, in the U-T plane, at zero doping, the phase diagram of the frustrated Hubbard model displays a region where two mean-field solutions, one metallic- and one insulating-like, can be obtained. This region is delimited by the $U_{c1}(T)$ and $U_{c2}(T)$ bifurcation lines. Within this region, there is a first-order MIT line [8,9] where the free energies of the two solutions cross. The line starts out at U_{c2} for $T = 0$ and ends at a finite temperature second-order critical point $(U_{\mathrm{MIT}}, T_{\mathrm{MIT}})$, which has the character of a regular Ising bifurcation with a rapid variation of the susceptibility connected to the double occupancy [10,11]. At higher temperatures, the $U_{c1}(T)$ and $U_{c2}(T)$ lines become crossover lines, which have a well-defined experimental significance [12].

The zero temperature aspects of the doping driven MIT were studied in [13]. It was shown that in the U-μ plane ($T = 0$) there are two solutions within a region bounded by the curves $\mu_{c1}(U)$ where the insulating solution disappears, and $\mu_{c2}(U)$ where the metallic state disappears. At $T = 0$, one finds that the μ_{c1} line ends at $U = U_{c1}$ and $\mu = U/2$, and the μ_{c2} line ends at $U = U_{c2}$ and $\mu = U/2$. The finite temperature aspects of the doping driven Mott transition have not been investigated thus far. This is the subject of our paper.

Our main interest is the behavior of the charge compressibility near the doping driven Mott transition in the paramagnetic phase at finite temperatures. We will not

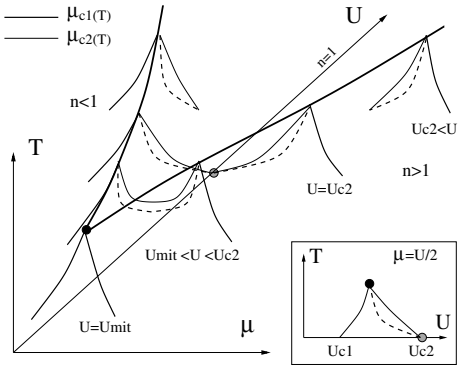

FIG. 1. Schematic phase diagram for the Hubbard model. The cross sections shown are on the T-μ plane for different values of U. μ_{c1} and U_{c1} are the chemical potential and interaction, respectively, at which the insulating solution gets destroyed. μ_{c2} and U_{c2} are those at which the metallic solution gets destroyed. The dashed lines denote the first-order transition. The thick solid lines denote the second-order lines where the compressibility diverges. The black circle at $(U_{\mathrm{MIT}}, T_{\mathrm{MIT}})$ denotes the second-order transition at $n = 1$. The $U_{c2}(T = 0)$ end point is denoted with a grey circle. Inset: phase diagram at particle-hole symmetry $\mu = U/2$ ($\tilde{\mu} = 0$). Solid lines denote $U_{c1}(T)$ (left) and $U_{c2}(T)$ (right).

consider the effects of long range order. Furukawa and Imada [14] pointed out that the compressibility diverges at the density driven MIT in two dimension at $T = 0$. This behavior has been also observed on other models of correlated electron systems, indicating that this phenomenon is quite general [15]. It is important to understand the physical origin of this result, and to see if it is realized in the DMFT solution of the Hubbard model. The previously investigated bifurcations within the DMFT have either a finite charge compressibility, such as in the $T = 0$ density driven MIT, or a vanishing charge compressibility, as in the $T = 0$ correlation driven MIT.

Our study of the neighborhood of the Mott transition is relevant to materials which have a finite temperature isostructural phase transition such as cerium (Ce). This can be seen by generalizing the derivation of the Landau free energy of [11]. Near the second-order end point, the free energy of more complicated models would have the same form as that studied in our paper.

We focus on the m-band degenerate Hubbard model:

$$H - \mu N = -\frac{t}{\sqrt{z}} \sum_{\langle ij\rangle m\sigma} c^{\dagger}_{im\sigma} c_{jm\sigma} + \frac{U}{2} \sum_{i,m,m'\sigma} n_{im\sigma} n_{im'-\sigma} + \frac{U}{2} \sum_{i,m\neq m'\sigma} n_{im\sigma} n_{im'\sigma} - \mu \sum_{im\sigma} n_{im\sigma} . \quad (1)$$

The first term describes the hopping between nearest neighbors $\langle ij\rangle$ on a lattice with coordination number z. $m, m' = 1, 2$ are the band indices and $\sigma = \uparrow, \downarrow$ labels the spin index. The parameter U is the energy cost associated with having a double occupancy on each site. t and U are assumed to be independent of the band indices. In the limit of infinite dimensions, $z \to \infty$, this model can be mapped onto a single-impurity Anderson model (SIAM) supplemented by a self-consistency condition [4]. The DMFT equation of the model reads

$$t^2 G_{m\sigma}(i\omega_n)[\Delta, \alpha] = \Delta(i\omega_n), \quad (2)$$

where ω_n are the fermionic Matsubara frequencies, $G_{m\sigma}$ is the impurity Green's function, and Δ is the hybridization function of the SIAM. Here, α denotes a control parameter such as T, U, or μ. We adopt a semicircular density of states, $\rho(\epsilon) = (\frac{2}{\pi D})\sqrt{1 - (\epsilon/D)^2}$, where the half-bandwidth $D = 2t = 1$ is our unit of energy.

We propose a schematic phase diagram (Fig. 1) for the one-band Hubbard model. The figure shows regions of coexisting solutions in cross sections of constant U in the (U, T, μ) parameter space. The $\tilde{\mu}$ axis starts at zero doping, thus $n = 1$ on the (U, T) plane where $\tilde{\mu} = 0$, which for the one-band model is $\tilde{\mu} = \mu - U/2$. At larger values of U, the regions of coexisting solutions are two triangles, one for $n < 1$ and the other for $n > 1$. These triangles are delimited by the $\mu_{c1}(T)$ and $\mu_{c2}(T)$ lines which correspond to the vanishing of the insulating and the metallic solutions, respectively. As U decreases, the triangular regions approach each other and fully merge at $U = U_{\mathrm{MIT}}$. Further lowering U makes the single triangular region diminish until $U = U_{c1}(T = 0)$, where it vanishes. Within the triangular regions, two mean-field solutions can be obtained, therefore a first-order transition exists where their free energies cross. This leads to a first-order transition *surface* between an insulating and a metallic-like state at finite T. The intersections of this surface with the constant-U cross sections are first-order lines that we denote by the dashed lines in Fig. 1. At $T = 0$ within the coexistence regions (the base of the triangles), the metallic state is always stable, thus one can cross the first-order surface towards the insulator by either increasing T, increasing U, or decreasing the doping.

At finite T, the two solutions merge where the triangular regions end. Hence, there is a *line* of second-order transitions where the first-order surface ends. This is denoted by the thick solid line in Fig. 1. The doping is small but nonzero along this line except at $U = U_{\mathrm{MIT}}$ where $n = 1$. As we shall show below, an interesting result of our work is the divergence of the compressibility on this line of second-order transitions.

For the two-band model, the phase diagram is qualitatively similar to the one-band case, except that the pairs of triangles at a given U do not have the same height due to the absence of particle-hole symmetry. The presence of a coexistence region and a first-order phase transition in the two-band model was apparent in earlier Monte Carlo calculations [16]. This also follows from the form of the Landau functional of this problem [5], which is similar for the one-band and the multiband situations. The finite temperature and general chemical potential aspects of this problem, and the behavior of the compressibility, had not been discussed previously in the literature.

We now turn to our numerical results that support this scenario. We solved the DMFT equation (2) iteratively using quantum Monte Carlo (QMC) methods in the (U, T, μ) parameter space for the one- and the two-band models. In Fig. 2 we show the doping (per spin) $\delta = \langle n\rangle - 1/2$ as a function of the chemical potential μ obtained from QMC calculations with $\Delta\tau = 0.5$ in the one-band case. The interaction value $U = 2.46$ is chosen to be within the small region delimited by $U_{\mathrm{MIT}} < U < U_{c2}(T = 0)$ [10]. In the lower panel, we show the results at several temperatures above the critical temperature T_{MIT} where only one solution exists. As T is decreased and T_{MIT} is approached, the curves show a fast crossover from small to large compressibility. The sigmoidal shape of the curve is a hallmark of the approach to a second-order critical point in Landau theory, as in the familiar Ising mean-field (IMF) model. In fact, upon further lowering T beneath T_{MIT}, two solutions are found to coexist, analogous to the IMF model case. The results are shown in the upper panel, where a

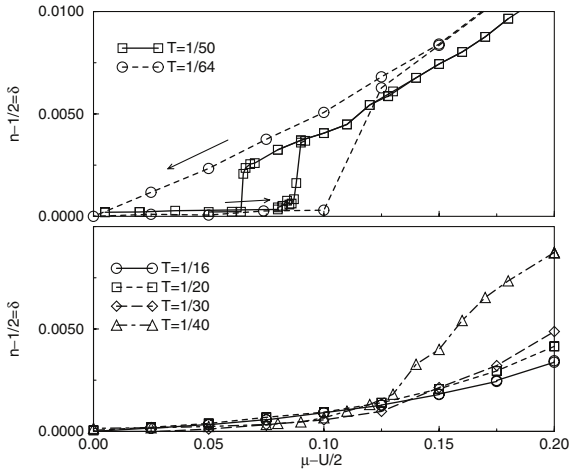

FIG. 2. Doping δ per spin as a function of the shifted chemical potential $\mu - U/2$ for various T. Lower panel: QMC data obtained at $T = 1/40, 1/30, 1/20, 1/16$ (right to left), all above T_{MIT}. Upper panel: Similar data at $T = 1/64$, $1/50$, below T_{MIT}. The arrows indicate a hysteresis-like cycle obtained by following the metallic and insulating solutions.

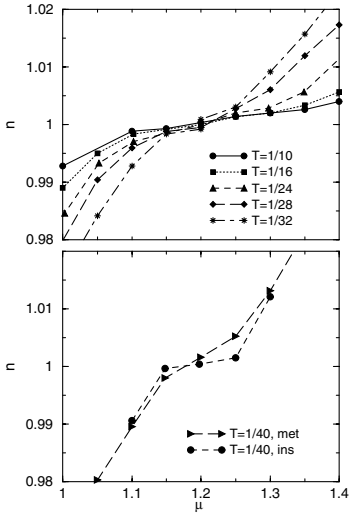

FIG. 3. Particle occupation n function of μ for different temperatures. in the two-band model at $U = 3.0$. In the upper panel, the temperatures are above the critical temperature while, in the lower panel, we see coexistence at $T < T_{\mathrm{MIT}}$.

hysteresis-like cycle is obtained. The cycle becomes larger at lower temperatures as the stability region of the solutions increases. At $T = 1/64$ we find that the metallic state persists all the way down to zero doping at $\mu = U/2$. This implies that, for $U_{\mathrm{MIT}} < U < U_{c2}$, the $\mu_{c2}(T)$ line does not go all the way down to $T = 0$ in contrast to the case when $U > U_{c2}$ (cf. Fig. 2).

To obtain the two solutions below T_{MIT}, we first start at high doping where only the metallic state exists, and then decrease μ as indicated by the left arrow in the upper panel of Fig. 2. We use a converged solution as the input seed for the next iteration. When the metallic solution disappears at μ_{c2}, a sudden drop in the occupation is seen. To obtain the other branch of the hysteresis loop, we begin with the insulating solution at $\mu = U/2$ ($n = 1$) and slowly increase μ, again using the previous converged solution as seed for the next value of μ. This state is essentially incompressible as n almost remains constant while increasing μ. The system is gradually doped until n jumps up at μ_{c1}, where the insulating state becomes unstable. This procedure can be used to map out the contour of the schematic phase diagram of Fig. 1 [17].

Similar behavior was found in the two-band model, and the results for the total occupation number n as a function of μ are shown in Fig. 3. The QMC calculation was performed at $\Delta\tau = 0.25$ and $U = 3.0$. At higher temperatures, only one solution is present, whereas on lowering T to $1/40$ both metallic and insulating solutions coexist.

A common feature that emerges from the models is that, in the regions where two mean-field solutions exist, the system has two different values of n for given T and μ. Furthermore, these two solutions have different free energies and the actual thermodynamic state of the system is that of minimum energy. Hence, a jump in the particle occupation is predicted at a first-order line. The determination of this line implies a precise calculation of the free energy which, in principle, is possible but technically hard and is outside the scope of the present work.

From the n versus μ curves in Figs. 2 and 3, we computed the numerical derivative of the particle number with respect to the chemical potential to obtain charge compressibility κ. The results for κ^{-1} as a function of the temperature above T_{MIT} (Fig. 4) indicate that $\kappa^{-1} \to 0$ as we approach the critical (thick solid) line in Fig. 1.

We also mention that in our simulations we observed characteristic effects of enhanced fluctuations and critical slowing down as the MIT is approached. Hence, simulations have to be done with extreme care, appropriately choosing the seeds for the iterative process and gathering many sample points for accurate statistics. In practice, we use up to $\sim 10^5$ Monte Carlo sweeps and hundreds of iterations to obtain converged solutions when we are close to the second-order critical line.

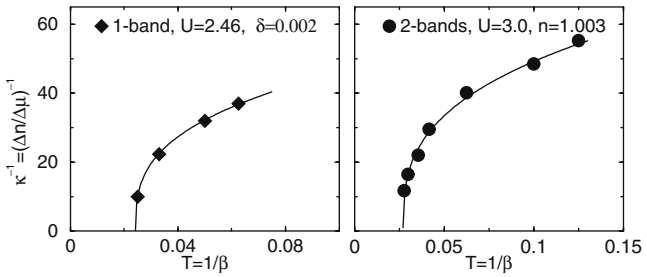

FIG. 4. The inverse compressibility κ^{-1}, at a constant doping as a function of T. Left: One-band model at $U = 2.46$ with doping $\delta = 0.002$. Right: Two-band model at $U = 3.0$ at $n = 1.003$. The solid lines are a guide to the eye.

We now present Landau theory arguments to support the idea of divergent compressibility at the Mott end point. The mean-field equation (2) can be obtained by differentiating the Landau functional [5],

$$F_{\mathrm{LG}}[\Delta] = -T \sum_n \frac{\Delta(i\omega_n)^2}{t^2} + F_{\mathrm{imp}}[\Delta], \qquad (3)$$

with respect to the hybridization $\Delta(i\omega_n)$ of the SIAM, which has the meaning of a Weiss field. $F_{\mathrm{imp}}[\Delta]$ is the free energy of the SIAM in the presence of a hybridization. The Green's function of the SIAM is $G(i\omega_n)[\Delta, \alpha] = (1/2T)\delta F_{\mathrm{imp}}/\delta\Delta$. This Landau approach was used to describe the Mott transition at half-filling [10,11].

As discussed in Ref. [11], the finite temperature Mott transition is a regular bifurcation point. On differentiating the Landau functional twice, we get a matrix of the form $-\delta_{nm} + M_{nm}$, where M_{nm} acquires a zero mode:

$$M_{nm} = \frac{t^2}{2T} \frac{\delta^2 F_{\mathrm{imp}}[\Delta]}{\delta\Delta(i\omega_n)\delta\Delta(i\omega_m)}\bigg|_{\mathrm{c.p.}}. \qquad (4)$$

We now make a small change in μ around the critical point and expand Eq. (2) to first order in $\delta\alpha = (\mu - \mu_c)$, $\delta\Delta = \Delta(\alpha_c + \delta\alpha) - \Delta(\alpha_c)$. We get

$$\frac{\delta\Delta(i\omega_n)}{\delta\alpha} = \sum_m \frac{1}{1 - M_{mn}} t^2 \frac{\partial G_{\mathrm{imp}}(i\omega_n)}{\partial\alpha}. \qquad (5)$$

From (2), the lattice occupation at any site which is identical to the local impurity occupation is related to the hybridization by $\langle n\rangle = (2T/t^2)\sum_n \Delta(i\omega n)$. Thus,

$$\frac{d\langle n\rangle}{d\mu} = 2\sum_n \left[\frac{1}{1 - M}\right] T \frac{\partial G_{\mathrm{imp}}(i\omega_n)}{\partial\mu}. \qquad (6)$$

Clearly, unless the derivative on the right-hand side of (6) is exactly orthogonal to the zero mode of the matrix M, the bifurcation condition leads to the singular behavior of the compressibility. The QMC studies shown above demonstrate that this orthogonality does not occur in general.

From the experimental viewpoint, we believe that our results highlight important aspects of the physics of the α-γ transition in Ce. The detailed description of the nonuniversal aspects of this material requires more elaborate models such as those studied by Held *et al.* [18]. However, the functional describing these complicated models near the finite temperature Mott transition would reduce to the one underlying the equations we studied. Hence, it is plausible that the behavior of the compressibility that we identified in our basic model applies to the α-γ transition of Ce as well. The divergence of compressibility in the Ce α-γ transition therefore has an electronic origin and can be understood from model calculations without involving lattice degrees of freedom (which would renormalize values of the critical points without changing qualitative features). In our data, we find a decrease in compressibility during the transition from the insulating to the metallic phase which is similar to what has been measured by Beecroft and Swenson in [19].

In summary, we presented a careful QMC study of the doping driven Mott transition within the DMFT. Our study unveils that the divergence of the compressibility is a generic feature of the finite temperature Mott end point. We understood this divergence in terms of an argument based on Landau theory, which indicates that these results are more general than the specific models for which the numerical studies were performed. Our results were found to be relevant to the Ce α-γ transition.

This research was supported by the Division of Materials Research of the National Science Foundation, under Grant No. NSF DMR 0096462, the Division of Basic Energy Sciences of the Department of Energy under U.S. DOE Grant No. DE-FG02-99ER45761. M. J. R. acknowledges support of Fundación Antorchas, CONICET (PID No. 4547/96), and ANPCYT (PMT-PICT1855).

[1] N. F. Mott, *Metal-Insulator Transitions* (Taylor & Francis, London, 1974).
[2] For a review, see M. Imada, A. Fujimori, and Y. Tokura, Rev. Mod. Phys. **70**, 1039 (1998).
[3] B. Johansson, Philos. Mag. **30**, 469 (1974).
[4] For a review, see A. Georges, G. Kotliar, W. Krauth, and M. J. Rozenberg, Rev. Mod. Phys. **68**, 13 (1996).
[5] G. Kotliar, Eur. J. Phys. B **11**, 27 (1999).
[6] R. Chitra and G. Kotliar, Phys. Rev. B **63**, 115110 (2001).
[7] W. F. Brinkman and T. M. Rice, Phys. Rev. B **2**, 4302 (1970).
[8] A. Georges and W. Krauth, Phys. Rev. B **48**, 7167 (1993).
[9] M. J. Rozenberg, G. Kotliar, and X. Y. Zhang, Phys. Rev. B **49**, 10 181 (1994).
[10] M. J. Rozenberg, R. Chitra, and G. Kotliar, Phys. Rev. Lett. **83**, 3498 (1999).
[11] G. Kotliar, E. Lange, and M. J. Rozenberg, Phys. Rev. Lett. **84**, 5180 (2000).
[12] M. J. Rozenberg, G. Kotliar, H. Kajueter, G. A. Thomas, D. H. Rapkine, J. M. Honig, and P. Metcalf, Phys. Rev. Lett. **75**, 105 (1995).
[13] D. S. Fisher, G. Kotliar, and G. Moeller, Phys. Rev. B **52**, 17 112 (1995).
[14] N. Furukawa and M. Imada, J. Phys. Soc. Jpn. **60**, 3604 (1991).
[15] M. Kohno, Phys. Rev. B **55**, 1435 (1997).
[16] Marcelo J. Rozenberg, Phys. Rev. B **55**, 4855 (1997).
[17] J. Joo and V. Oudovenko, Phys. Rev. B **64**, 193102 (2001).
[18] K. Held, A. K. McMahan, and R. T. Scalettar, cond-mat/0106599; C. Huscroft, A. K. McMahan, and R. T. Scalettar, Phys. Rev. Lett. **82**, 2342 (1999).
[19] R. I. Beecroft and C. A. Swenson, J. Phys. Chem. Solids **15**, 234 (1960).